Response behavior of ZrO_2 under swift heavy ion irradiation with and without external pressure

B. Schuster[a,b,*], F. Fujara[a], B. Merk[a,b], R. Neumann[b], T. Seidl[a,b], C. Trautmann[b]

[a] *Technische Universität Darmstadt, Hochschulstr. 6, 64289 Darmstadt*
[b] *Helmholtz Centre for Heavy Ion Reseach (GSI), Planckstr. 1, 64291 Darmstadt*

Abstract

In this study, we demonstrate that the combination of relativistic heavy ions with pressure can influence the phase behavior of ZrO_2 in ways none of those two extreme conditions alone could. The response behavior of ZrO_2 towards ion irradiation under different pressure conditions is investigated. ZrO_2 exposed to energetic particles is known to undergo a crystalline-to-crystalline phase transition from the monoclinic to the tetragonal phase. In agreement with earlier findings, this structural change requires also for heaviest ions, such as Au, Pb, and U, a multiple ion impact. If the irradiation is performed under high pressure, the monoclinic-to-tetragonal transformation occurs at a fluence that is more than one order of magnitude lower suggesting a single impact process. Raman measurements at ambient conditions and X-ray diffraction analysis of the samples irradiated under pressure revealed that the monoclinic-to-tetragonal transformation under pressure is not a direct process but involves a transition into the cubic high-temperature structure, before the tetragonal structure becomes stable under decompression. At even higher pressures, the additional ion irradiation forces ZrO_2 to transform to the higher orthorhombic-II phase that is far away from its stability field. straße

Keywords: Ion irradiation, High-pressure, Zirconia (ZrO_2), Phase transformation, Raman spectroscopy, Synchrotron X-ray

1. Introduction

On passing through a solid, swift heavy ions slow down and transfer their kinetic energy to the target electrons by ionization and excitation processes. In most solids, predominantly in insulators, the high, localized energy deposition leads to the formation of tracks, cylindrical damage regions (often consisting of amorphized material) a few nm in diameter surrounded by the pristine, undamaged matrix [1, 2]. Ion tracks are characterized by severe chemical, physical, and structural modifications. In non-amorphisable crystals, the track region contains numerous lattice defects [3, 4] and/or has undergone a transition to a different crystalline phase [5]. Until recently, most irradiations were performed at ambient pressure conditions. Here we describe a relatively new experimental approach by combining ion irradiation with high pressure [6]. Pressure applied during irradiation not only opens the access to a large variety of structural conformations of the starting material but also allows new routes for phase transitions within the *p-T* phase diagram. Additional pressure was shown to enhance or hinder certain radiation induced transformations [7, 8]. Conversely, ion irradiation can change the stability field of some materials [6, 9]. The exposure of pressurized samples to ion beams also provides insight how pressure-induced phase transitions in minerals may be affected by pre-existing damage and by the microstructure of the starting material. Recent results demonstrated that new structural phases may become accessible [7].

In this study we concentrate on ZrO_2 (zirconia) and its response to ion irradiation and pressure. Zirconia is known for its high fracture toughness, low thermal expansion, high refractoriness, high resistance to wear and corrosion, and especially chemical inertness. Because of these properties, ZrO_2 is one of the most important functional ceramics [10]. It is used, e.g., as inert fuel matrix in nuclear reactors [11, 12, 13] or as containment material for radioactive waste [14, 15]. Important for our experiments is the existence of several structural polymorphs and the fact that ion irradiation at ambient pressure leads to a structural transition from the monoclinic to the tetragonal phase [16]. Depending on pressure and temperature, zirconia has five known structural conformations: At ambient pressure and temperature conditions, ZrO_2 exists as a white powder in its monoclinic phase (also called baddelyte). At temperatures around 1170 °C, zirconia transforms to its tetragonal high-temperature form accompanied by a density increase of ~ 4-5 % [17]. At 2370 °C, a transformation to the cubic structure occurs, before melting sets in around 2700 °C [14]. Zirconia also exhibits two high pressure phases, but the exact boundaries are not well defined, although numerous groups (e.g. [18, 19, 20, 21, 22, 23]) have performed high-pressure experiments. The problem arises from the fact that high-pressure transitions often occur quite sluggishly and are not easily identified. At pressures between 4 and 7 GPa, the transition from the monoclinic to the first high-pressure phase, orthorhombic-I (space group Pbca, polyhedral coordination of seven), takes place [24, 19]. This displacive transition is well defined at room temperature and depends on the crystallite size. Even at pressures around 10 GPa and room

*Corresponding Author
Email address: bea.schuster@gsi.de (B. Schuster)

temperature, the transition is not complete, but residues of the monoclinic phase are detectable. The orthorhombic-I phase is not quenchable to ambient conditions. At elevated temperatures > 600 °C, the transition into a second high-pressure phase, orthorhombic-II (space group Pnma, polyhedral coordination of nine), takes place at 12.5 GPa. This transition is quite temperature dependent [18, 21, 24, 25]. At room temperature, it occurs between 25 and ≥ 30 GPa [18, 19, 20, 24, 25, 21, 26, 27, 28]. Because the ortho-I-to-ortho-II transition is reconstructive [29], it is not surprising that it becomes increasingly sluggish at ambient temperature and usually an excess pressure of > 10 GPa is needed for complete transformation [24]. This additional energy investment results in the increased stability of the orthorhombic-II phase, and is quenchable to ambient pressure [24, 25, 29]. The ortho-I-to-ortho-II transformation requires a significant reorganization of the cation and anion sublattices, increasing the coordination number of Zr^{4+} from seven to nine, and therefore the transformation kinetics are slowed down to the point of being irreversible at room temperature [21]. At ambient pressure, the radiation response of zirconia has been studied extensively for low-energy ions at room [30, 31, 32, 33] and cryogenic [13] temperatures, as well as for swift heavy ions [5, 34, 35, 36, 37, 38, 39]. All cited experiments showed that for very high ion fluences a structural phase transition from the monoclinic to the high-temperature tetragonal phase occurs. For experiments performed with low-energy ions in the nuclear stopping regime (e.g. Ge, Kr, or Xe-ions of energy around 300 keV), the transformation occurs only in a surface layer of few hundred nm [33] and requires fluences around 10^{18}-10^{19} ions/cm^2 [30]. For swift heavy ions with high electronic stopping (Ni, Ge, Kr, I, and Xe of energies up to about 10 MeV per nucleon (MeV/u)), the monoclinic-to-tetragonal transition requires a critical energy loss of 12 keV/nm [40] and saturates at fluences above 1×10^{13} ions/cm^2 [34], much lower than for beams in the elastic collision regime. Compared to the earlier results, all irradiations presented here were performed with heavy ion species Au, Pb, and U. Moreover, we concentrate on how pressure influences the ion-induced damage process by comparing ZrO_2 irradiated under ambient and various high pressures.

2. Experimental

The irradiations of zirconia samples were performed at two different beamlines of the accelerator facilities at the GSI Helmholtz Centre for Heavy Ion Research in Darmstadt, Germany. Experiments at ambient pressure were carried out at the UNILAC (Universal Linear Accelerator) using ^{197}Au, ^{208}Pb, and ^{238}U ions of 11.4 MeV/u, while irradiations of samples pressurized in diamond anvil cells required energies between 150 and 200 MeV/u available at the heavy ion synchrotron SIS. In both cases, the stopping process of the ions is dominated by electronic excitation, i.e. the nuclear energy loss via elastic collisions of projectiles with atoms of the sample can be neglected. All irradiations were performed at room temperature and under normal beam incidence. For the irradiation at ambient pressure, powder samples (purchased from Sigma-Aldrich)

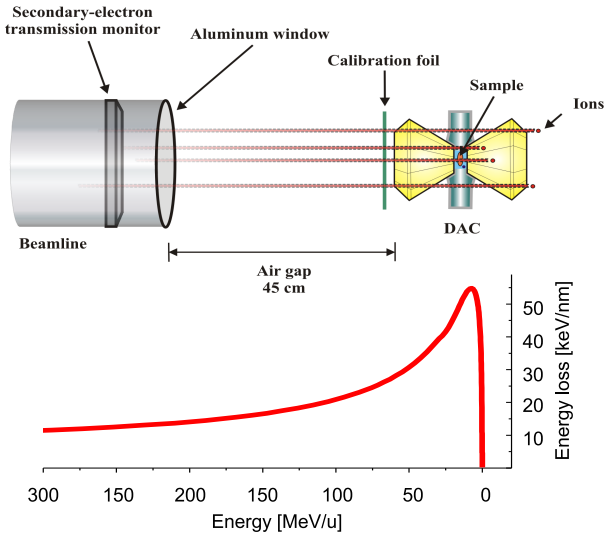

Figure 1: Schematic of sample irradiation inside a diamond anvil cell at the heavy ion synchrotron SIS (not to scale). Before reaching the sample, the beam exits through an Al window and travels across 45 cm of air and ~ 2 mm of diamond. The initial ion energy is selected such that the energy loss maximum lies thightly behind the sample.

were fixed at thin indium foils. During ion exposure, the beam flux and fluence were controlled via a secondary electron transmission monitor (calibrated with a standard Faraday cup) that reduces the initial beam energy to 11.1 MeV/u. The range of all ions in ZrO_2 was ~ 60 μm [41]. The ion flux was limited to ~ 2-5×10^8 ions/cm^2 to avoid macroscopic sample heating. Fluence series covered values from 1×10^{11} up to 1×10^{13} ions/cm^2. The averaged electronic energy loss $(dE/dx)_e$ within the sample was 40 keV/nm for Au, 42 keV/nm for Pb, and 53 keV/nm for U ions, calculated with the SRIM 2008 code [41]. All irradiation parameters are listed in Table 1.

For high pressure application, we used diamond anvil cells (DAC) consisting of two opposing diamonds with the sample compressed between the culets. Based on the simple principle of $P = F/A$, the pressure P is obtained by exerting a force F on the small culet faces of area A of the two diamonds [42]. DACs routinely provide access to pressures as large as several tens of GPa and more. Being a hand-held device of low weight, they can easily be transported to different experimental sites [43]. A scheme of the basic principle of the DAC irradiation is shown in Fig. 1.

For pressurization, monoclinic ZrO_2 powder was inserted in the central aperture (diameter 150 μm) of a stainless steel gasket mounted between two diamonds. To ensure hydrostatic conditions up to (10 ± 0.5) GPa a methanol:ethanol:water mixture (16:3:1) was filled into the sample chamber as an optically transparent pressure medium [44]. In addition, a small ruby crystal (~ 5-10 μm) was inserted acting as pressure gauge before and after irradiation. The pressure is determined by recording the wavelength of the red fluorescence line of the ruby crystal, which shifts to lower energies with increasing pressures but remains unaffected by the irradiation up to fluences above >

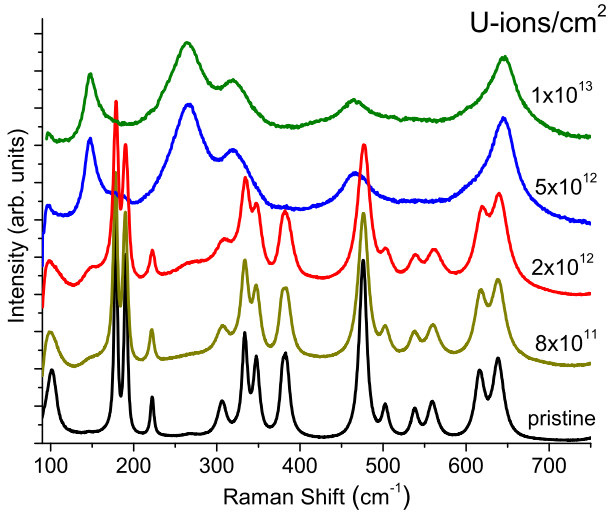

Figure 2: Raman spectra of ZrO_2 irradiated at ambient pressure with 11.1 MeV/u U-ions for various fluences.

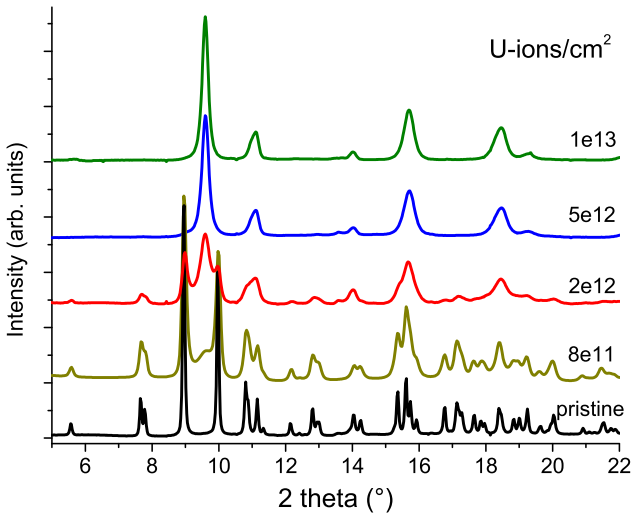

Figure 3: X-ray spectra of ZrO_2 irradiated at ambient pressure with 11.1 MeV/u U-ions for various fluences (same sample as in Fig. 2).

1-2×10^{12} U-ions/cm^2 [45, 46, 47].

Irradiations of pressurized samples were performed at the heavy-ion synchrotron SIS providing a pulsed beam (pulse rate 0.3 Hz). The initial kinetic energy of the Au and U ions was about 150 - 200 MeV/u, sufficiently high that the ions passed through the first diamond (∼ 2 mm) of the DAC and still had about 30 MeV/u when reaching the sample. The electronic energy loss of U ions in the sample is about ∼ 40 keV/nm, but this value is not very precise because of the uncertainty of the beam energy after the passage through the thick diamond [48] and due to nuclear fragmentation of the projectiles. A scheme of the DAC irradiation together with the energy loss as a function of the kinetic energy of the ions is shown in Fig. 1. The initial energy is selected such that the energy loss in the sample is close to the energy loss maximum (Bragg peak). On their passage through the first diamond and sample, the ions deposit their energy and are finally stopped in the second diamond. Different experiments with low (∼ 1×10^{11} ions/cm^2) as well as high (2×10^{12} ions/cm^2) fluences were performed.

X-ray diffraction measurements of the pressurized samples were performed at the P08 beamline of PETRA at the German Electron Synchrotron (DESY) in Hamburg with a beam energy of (25.054 ± 0.005) keV (λ = 0.49467 Å) and an X-ray spot of ∼ 50 μm in diameter. The energy selection was accomplished by using a double-crystal monochromator with Si crystals. The Debye-Scherrer rings were recorded with a Perkin-Elmer detector with a 16 bit digital resolution of 200 μm pixels and an image size of 2048×2048 pixels. The diffraction image was integrated into two-dimensional patterns with the program Fit2D [49]. The configuration parameters of the experimental setup were calibrated with a cerium dioxide (CeO_2) standard. The XRD patterns were refined by the Rietveld method using the MAUD [50] and GSAS [51] software.

All irradiated samples were also analyzed by confocal Raman spectroscopy with a commercial 180° Raman spectrometer (Horiba Jobin Yvon HR800). The instrument has a grating of 1800 grooves/mm, a spectral resolution of about 0.01 nm, and an excitation wavelength of λ = 632.8 nm from a He-Ne laser. The spot size of the laser beam was about 1 μm^2. Background correction and mathematical fitting of the bands were done using the FITYK 0.9.7 software [52].

Unfortunately, Raman spectroscopy could not be performed under pressure because the ion irradiation changed the color of the diamonds into dark green, almost black. The samples were thus analyzed at ambient pressure, outside the DAC. All irradiations and measurements were performed at room temperature.

3. Results and Discussion

3.1. Irradiations at ambient pressure

Raman spectra of ZrO_2 irradiated at ambient pressure with various fluences of U ions are displayed in Fig. 2. Pristine ZrO_2 has 14 dominant Raman lines at 100, 178, 190, 222, 305, 334, 348, 382, 476, 503, 537, 560, 616, and 640 cm^{-1} corresponding to the low-symmetric monoclinic structure. For fluences up to 1×10^{12} U-ions/cm^2 the Raman spectra remain almost unchanged. At fluences around 2×10^{12} U-ions/cm^2, small modifications become visible, such as the decrease of the band at 100 cm^{-1} and merging of the double band structures at 340, 550, and 630 cm^{-1}. At 5×10^{12} ions/cm^2, new broad bands appear at 148, 265, 465, and 640 cm^{-1} which are assigned to the tetragonal phase of ZrO_2 [34, 53, 39]. The transformation mainly proceeds in a fluence regime between 2 and 5×10^{12} U-ions/cm^2, while above this range the changes are only marginal. Interestingly, we always identified a small contribution of the monoclinic phase. For the sample irradiated with 1×10^{13} U-ions/cm^2, e.g., the tetragonal fraction is limited to (90.1 ± 4.4) %. In agreement with previous measurements [9, 5], the transformation from monoclinic to tetragonal is obviously never complete. It is important to point out that the tetragonal structure of ZrO_2 obtained by simple temperature increase is not stable at room

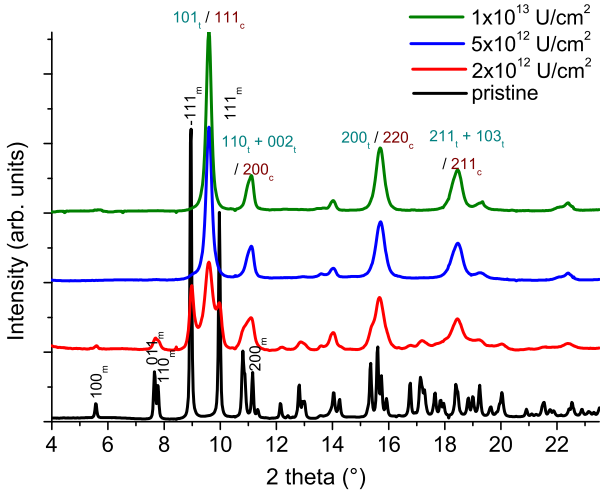

Figure 4: Evolution of the concentration of the tetragonal phase versus fluence for three different ion species (Au, Pb, U) deduced from the Raman data. The solid curves are best fits of Eq.(3) to the experimental data using a triple impac process (n = 2). For comparison, fits to the Au data with double impact (n = 1, dashed line) and single impact (n = 0, dotted line) are shown.

temperature. Therefore, the production route via ion irradiation is unique in the sense that it can not only provoke the transformation from the monoclinic to the tetragonal phase, but that this high-temperature phase is stable down to ambient temperature. Within our observation time of ~ 2 years, the tetragonal phase remained stable. Complementary X-ray diffraction measurements were performed on samples irradiated with 11.1 MeV/u U-ions (Fig. 3). The pristine sample exhibits its strongest peaks at 8.95 ° corresponding to the $(-111)_m$ reflection and at 9.97 ° corresponding to the $(111)_m$ reflection of the monoclinic structure. The calculated lattice parameters for pristine ZrO_2 are a = (5.296 ± 0.006) Å, b = (5.094 ± 0.007) Å, c = (5.326 ± 0.006) Å, and an angle β = 99.40 °. Similar to the Raman data, for fluences ≥ 1×10^{12} U-ions/cm^2 the monoclinic bands start to deteriorate and a new reflection at 9.60 ° appears that belongs to the $(101)_t$ reflection of the tetragonal phase. The calculated lattice parameters for the tetragonal structure are a = (3.630 ± 0.006) Å, and c = (5.139 ± 0.013) Å. ZrO_2 is one of the rare materials in which the high-temperature phase has a higher density than the room temperature phase, which leads to the fact that the monoclinic-to-tetragonal transition is accompanied by a density increase of ~ 5 % [17]. To shed more light on the mechanism of this transformation, Raman spectra of similar fluence series were analyzed for samples irradiated with 11.1 MeV/u Au, Pb, and U ions. To quantify the contribution of the monoclinic and tetragonal phases, we evaluated the intensity ratio (X_m) of the different Raman bands at 178, 190, and 148 cm^{-1}. The background was considered by subtracting the baseline between ~ 125 and ~ 205 cm^{-1}. The monoclinic fraction was calculated by applying the formula by Kim et al [53].

$$X_m = \frac{I_m(178\ cm^{-1}) + I_m(190\ cm^{-1})}{I_m(178\ cm^{-1}) + I_m(190\ cm^{-1}) + I_t(148\ cm^{-1})} \quad (1)$$

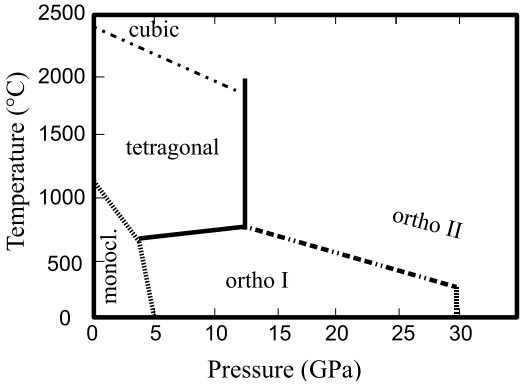

Figure 5: P-T phase diagram of ZrO_2 adjusted from [24]. Dashed lines are transitions under discussion.

For all tested ion species, the tetragonal fraction (100-X_m) in % plotted versus the ions fluence shows a sigmoidal evolution (Fig. 4). Such a behavior is commonly observed for non-amorphisable ceramics at ambient temperature [54, 55] and typically ascribed to a two or multiple impact damage process. This is in contrast to amorphisable materials where each ion produces an individual amorphised track of radius r and cross section $\sigma = r^2\pi$. For such a single impact process, the fraction of the transformed material A increases with fluence (Φ) according to the following exponential law [56].

$$A(\Phi) = A(\infty)(1 - e^{-\sigma\Phi}) \quad (2)$$

where σ is the total damage cross-section given as an area, and $A(\infty)$ represents the fraction of transformed material at saturation.

Fitting this formula to our Raman data does not yield satisfactory results (see dotted line in Fig. 4). The monoclinic phase of ZrO_2 can obviously not be transformed into the tetragonal phase by the impact of single ions but needs pre-damaging by multiple ion impacts. The effect of damage superposition is described by the Gibbons cascade-overlap model [56, 54] with the following general expression in which n is the multiplicity of damage overlap:

$$A(\Phi) = A(\infty)\left[1 - \left(\sum_{k=0}^{n} \frac{(\sigma\Phi)^k}{k!}\right) e^{-\sigma\Phi}\right] \quad (3)$$

For all ion species, we find best agreement with our data for a double-overlap situation (n = 2) represented by the solid lines in Fig. 4. The results of the fits are $A(\infty)$ = (93.7 ± 4.1) %, σ = (8.69 ± 0.21) ×10^{-13} cm^2 for U-ions, $A(\infty)$ = (91.3 ± 4.0) %, σ = (6.18 ± 0.32) ×10^{-13} cm^2 for Pb-ions, and $A(\infty)$ = (89.9 ± 4.7) %, σ = (5.04 ± 0.18) ×10^{-13} cm^2 for Au-ions. As has been reported in the literature (e.g. [34, 33]), the transformation is never complete but saturates at around 90 %. Assuming that the damage cross section σ can be described by a homogeneously damaged cylinder with a cross section $\sigma = \pi r^2$, the following track radii can be deduced: r = (5.3 ± 0.2) nm for U-ions, (4.4 ± 0.2) nm for Pb-ions, and (4.0 ± 0.2) nm for Au-ions. The results give evidence that heavy-ion irradiation at

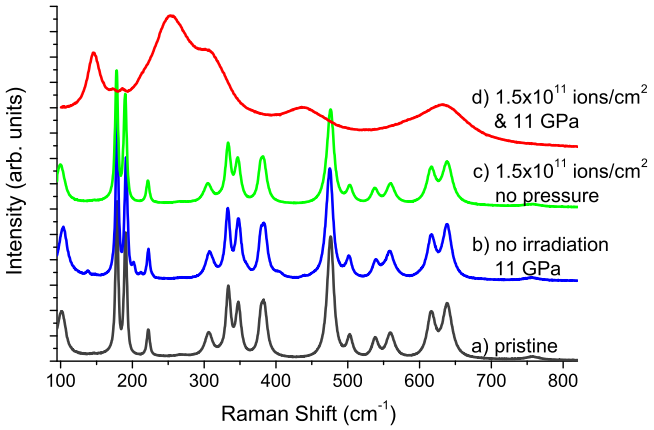

Figure 6: Raman spectra at ambient conditions of different ZrO_2 samples: (a) pristine, (b) pressurized without irradiation, (c) irradiated with 1.5×10^{11} U-ions/cm^2 but without pressure, (d) irradiated with 1.5×10^{11} U-ions/cm^2 at a pressure of (11.0 ± 0.3) GPa.

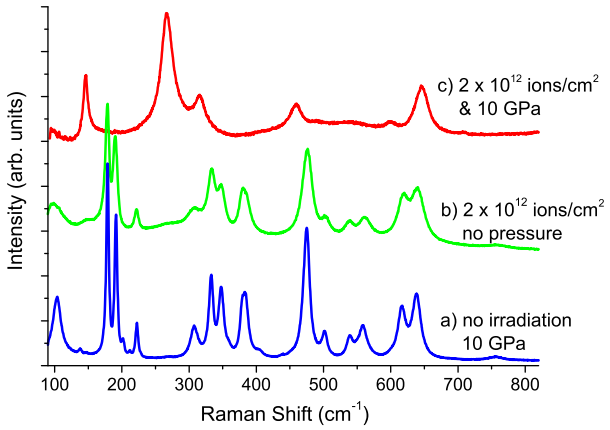

Figure 7: Raman spectra at ambient conditions of different ZrO_2 samples: (a) pressurized to 10.5 GPa but not irradiated, (b) irradiated with 2×10^{12} U-ions/cm^2 but without pressure, (c) irradiated with 2×10^{12} U-ions/cm^2 under pressure of (10.3 ± 0.3) GPa.

ambient pressure induces a structural change into the tetragonal phase only if the structure is pre-damaged by overlapping tracks. For U-ions, double track coverage requires fluences of about 2×10^{12} ions/cm^2. Above this fluence, each following ion hits a pre-damaged region, and transforms the damaged monoclinic structure into the tetragonal phase. This agrees nicely with the observed results.

3.2. High-Pressure Irradiations

Samples irradiated under high pressure and analyzed after pressure release show quite different results. When compressing ZrO_2 hydrostatically up to (11.0 ± 0.3) GPa, it remains no longer in the monoclinic structure but is mainly transformed into the first high-pressure orthorhombic-I phase (see Fig. 5). The pressurized sample was irradiated with a rather low fluence of 1.5×10^{11} U-ions/cm^2. After releasing the pressure, the sample was carefully analyzed by Raman spectroscopy applied to different sample locations. As described earlier in [9], some regions exhibit no change at all, whereas other regions are completely transformed into the tetragonal phase. In total, the fraction of completely transformed regions is ~ 10 % (see Fig. 6 (d)). This corresponds well to an area damaged by single ion impacts at a fluence of 1.5×10^{11} U-ions/cm^2 assuming a track radius of 5.3 nm. This is in clear contrast to the unpressurized reference sample, irradiated under the same conditions (Fig. 6(c)), that shows no deviation from a pristine sample at this low fluence. In transformed regions, the tetragonal fraction is 85.3 % as estimated by means of Eq. (1). Pressure alone as origin for the tetragonal fraction can be excluded, since the orthorhombic-I high-pressure phase is not quenchable as demonstrated by the unirradiated pressure reference sample (Fig. 6 (b)) which shows no significant difference towards the pristine sample besides some small residues around 200 cm^{-1}. Ion irradiation under pressure obviously allows a single ion impact to induce the phase transitions.

To further investigate the radiation response of pressurized ZrO_2, the experiment was repeated with a sample pressurized at (10.3 ± 0.3) GPa but exposed to a larger fluence of 2×10^{12} U-ions/cm^2, which is high enough to completely cover the area with ion hits. The Raman spectrum of this sample together with the spectra of a pressurized non-irradiated sample and a sample irradiated at ambient conditions are shown in Fig. 7.

Under high fluence, the pressurized sample exhibits an almost complete transformation into the tetragonal phase (see Fig. 7 (c)). Residues of the monoclinic bands at 178 and 190 cm^{-1} are barely visible. While for the experiment with lower fluence (1.5×10^{11} U-ions/cm^2) only ~ 10 % of the sample showed this strong transformation, this sample irradiated with 2×10^{12} U-ions/cm^2 is completely changed. The tetragonal fraction of the pressure-irradiated sample is (91.2 ± 3.4) %, whereas the fraction for a sample also irradiated with 2×10^{12} ions/cm^2 at ambient pressure is only (6.3 ± 0.8) % (see Fig. 7 (b)). It seems obvious that under pressure the monoclinic-to-tetragonal phase transformation is induced by a single ion not requiring predamaging.

With increasing pressure, the temperature necessary for the monoclinic-to-tetragonal transition decreases from ~ 1000 to ~ 600 °C (see Fig. 5) at around 4 GPa. In our previous work [9], we ruled out that the lower transition temperature of the ortho-I-to-tetragonal transition compared to the monoclinic-to-tetragonal transition is the decisive parameter. At pressures of 4.3 and 7.6 GPa, no enhanced radiation response appeared. So we can assume that the lower phase transition temperature is not the driving force behind the strong transformation behavior. As mentioned earlier, the irradiations of pressurized and pristine material are quite different, since we start with the denser orthorhombic-I phase. At ambient conditions, ZrO_2 has a density of 5.70 g/cm^3. Via Rietveld refinement, we determined the density of ZrO_2 at 10 GPa to be (6.04 ± 0.13) g/cm^3. The small density increase changes the electronic energy loss of

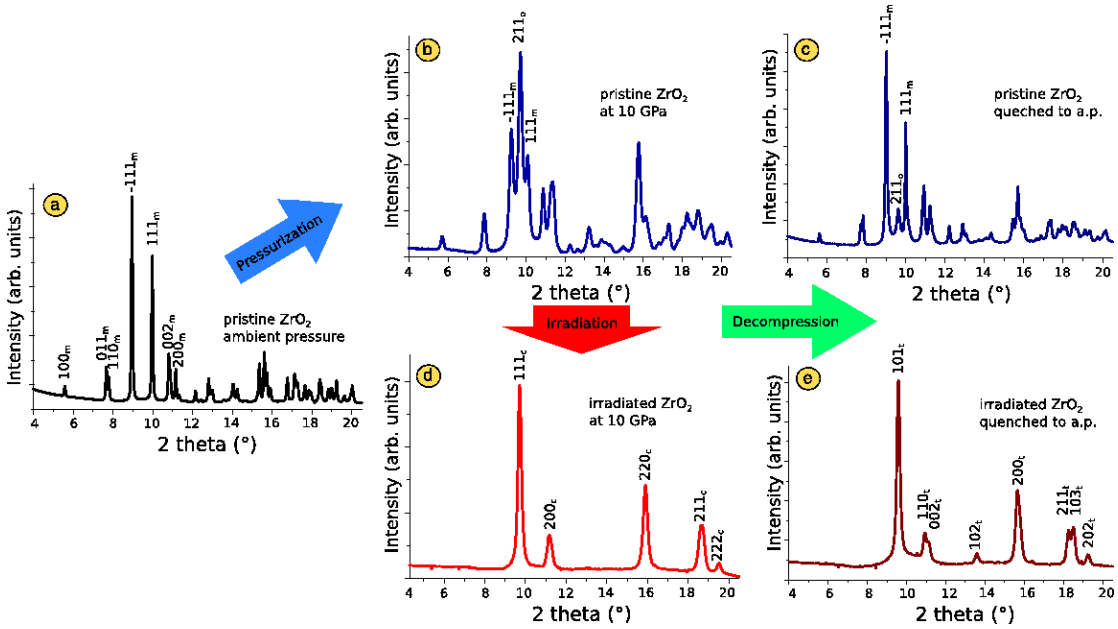

Figure 8: X-ray diffraction spectra of different stages of the experiment. At ambient conditions ZrO_2, shows peaks of the monoclinic structure (a). Pressurized to 10 GPa, new reflections which belong to the ortho-I phase appear as a mixture of monoclinic/ortho-I (b). Additional irradiation with 2×10^{12} U-ions/cm^2 provokes a transformation into the cubic phase (d). When releasing the pressure, the unirradiated sample transforms back into its monoclinic form (c), whereas the irradiated sample transforms into the tetragonal structure and remains stable in this phase also at ambient pressure (e).

U-ions in ZrO_2 only slightly from 37.3 to 39.3 keV/nm at an energy of 30 MeV/u. A density effect can therefore also be ruled out as possible influence, since the small energy loss difference of 2.2 keV/nm can be neglected considering that the ambient-pressure experiment performed at the UNILAC provided an energy loss of 53.2 kev/nm [41] and did not reveal any phase transition for fluences $\leq 2\times10^{12}$ ions/cm^2.

As discussed in the previous section, at ambient conditions one ion alone does not suffice to induce the structural phase transformation in ZrO_2, making a multiple impact mechanism reasonable. Several groups who investigated the radiation induced phase transition for low as well as high energy ions [36, 33, 40] explained the multiple impact mechanism by the production of oxygen vacancies. The presence of oxygen vacancies is considered as a requirement for a thermally induced phase transition [57]. Also in the case of tetragonal zirconia, artificially stabilized by addition of soluble oxides (e.g. Y_2O_3, MgO, CaO), the structure remains in the high-temperature phase because the dopants create oxygen vacancies for every unit of the dopant. The additional oxygen vacancies displace the remaining oxygen ions from their equilibrium position in the tetragonal phase, so that the tetragonal-to-monoclinic transformation is suppressed [58]. Under ion irradiation, probably a large number of oxygen vacancies is produced [59]. If they accumulate into vacancy clusters, the free volume can induce significant stress in the crystal that may relax via a phase transition [55]. Calculations showed that oxygen vacancies induce a strong local strain field in their neighborhood [60]. Using Landau's theory of phase transitions [61], Simeone et al. [37, 36] explained the transformation mechanism by also considering a local strain field induced by vacancies. Because they lower the critical transition temperature when reaching a certain threshold value. With respect to the free energy, the new crystalline phase is energetically the most favorable atomic configuration. The mechanism for ambient irradiations of ZrO_2 can be explained by the need to provide sufficient defects and strain by relatively high fluences. By hitting a pre-damaged region, further ion impacts then induce the transformation from defective monoclinic structure into the tetragonal phase. Such a mechanism would also explain why lower fluences are sufficient for the transformation at high pressure. The externally applied pressure provides internal stress within the sample, taking over the part of the first step of the ion impacts. We assume that at pressures < 7.6 GPa the strain field is too small to trigger the transition, explaining why at lower pressures the sample did not transform into the tetragonal phase.

Additional information on the transformation mechanism can be gained by the investigation of the ZrO_2 sample irradiated with 2×10^{12} ions/cm^2 by looking at the material still under pressure. Figure 8 shows the diffraction spectra of pristine, pressurized, and irradiated samples inside the DAC before and after quenching. At ambient pressure, the sample is monoclinic (Fig. 8 (a)). Under pressure of 10.3 GPa, it changes to the high-pressure orthorhombic-I phase, clearly visible by the $(211)_o$ reflection at 9.70 ° (Fig. 8 (b)). The transition is not complete and about 38 % of the sample remain in the monoclinic phase, indicated by the $(-111)_m$ and $(111)_m$ reflections. If the sample rests at this pressure for one week and is then quenched to ambient pressure, it changes back to monoclinic (Fig. 8 (c)) with a contribution of about 10 % of the orthorhombic phase. The situ-

Ion	E_{init} (GeV)	dE/dx (keV/nm)	Fluence Φ (ions/cm^2)	Pressure (GPa)	Initial structure	Final structure	Radius (nm)
UNILAC beam							
^{238}U	2.64	53	0.05 - 1.0×10^{13}	ambient	mono	tetragonal for Φ ≥ 5×10^{12}	5.3
^{208}Pb	2.31	42	0.05 - 7.5×10^{12}	ambient	mono	tetragonal for Φ ≥ 7×10^{12}	4.4
^{197}Au	2.19	40	0.05 - 1.8×10^{13}	ambient	mono	tetragonal for Φ ≥ 1×10^{13}	4.0
SIS beam							
^{238}U	7.14	39	1.5×10^{11}	11.0 ± 0.3	ortho-I	strong tetragonal regions	
^{238}U	7.14	37	1.5×10^{11}	ambient	mono	mono	
^{238}U	7.14	39	2.0×10^{12}	10.3 ± 0.3	ortho-I	cubic (10 GPa), tetragonal (ambient)	
^{238}U	7.14	37	2.0×10^{12}	ambient	mono	mono	
^{238}U	7.14	≥ 39	1.5×10^{12}	23 ± 1.0	ortho-I	ortho-II	
^{238}U	7.14	≥ 39	1.5×10^{12}	38 ± 2.0	ortho-II	ortho-II	
^{238}U	7.14	≥ 39	1.5×10^{12}	70 ± 4.0	ortho-II	ortho-II	

Table 1: Irradiation and pressure parameters for all samples irradiated at the UNILAC at ambient pressure and for those irradiated at the SIS under high pressure. The table summarizes the crystalline strcutures before and after irradiation, as determined at ambient conditions.

ation is very different for the sample irradiated under a pressure of 10 GPa. Instead of the expected tetragonal structure, we find the second high-temperature cubic phase of ZrO_2 evidenced by the $(111)_c$ reflection at 9.72°, $(200)_c$ reflection at 11.17°, and $(220)_c$ reflection at 15.90° (Fig. 8 (d)). Rietveld refinement yields a lattice constant of a = (5.072 ± 0.002) Å. This stage could not be derived from the Raman data performed at ambient pressure (see Fig. 7). Surprisingly, during pressure release the cubic structure does not transform into the expected ambient monoclinic but instead into the tetragonal structure. This XRD result is in agreement with our observation by means of Raman spectroscopy at ambient pressure. From the information obtained from the XRD data, it is difficult to assign the phase because of the fact that the tetragonal and cubic phases are very similar, and the structure identification relies on small differences. When releasing the pressure, the cubic peak at 11.17° splits into two individual peaks belonging to $(110)_t$ at 10.94° and $(002)_t$ at 11.13° of the tetragonal phase. Similar splittings can be observed at larger diffraction angles, e.g. $(211)_t$ and $(103)_3$ at around ∼ 18.5°. Also the $(102)_t$ reflection appearing at 13.57° is a clear indication of the tetragonal phase. During decompression, the cubic phase remains stable down to ∼ 3 GPa and then undergoes a sudden change into the tetragonal phase within the last decompression step. Unfortunately, unambiguous identification of these two phases by Raman spectroscopy is also very difficult, because the Raman band of cubic ZrO_2 expected at 620 cm^{-1} is hidden below the broad band at 640 cm^{-1} from the tetragonal structure.

3.3. Irradiations at very high pressures

Up to now, irradiations performed at ambient conditions and pressures up to 11 GPa under hydrostatic conditions were dicussed. For pressures up to 12.5 GPa, the temperature path comprises a transition from monoclinic → tetragonal → cubic (see Fig. 5). The question arises what happens, if ZrO_2 is irradiated at higher pressures where the previously discussed transition path is no longer possible. Three additional pressure irradiation experiments were performed at extreme pressures of 23, 38, and 70 GPa. The sample at 23 GPa has the orthorhombic-I structure, while the samples at 38, and 70 GPa are well within the stability field of the second high pressure phase orthorhombic-II. Starting at the orthorhombic-II phase, the beam-induced transformation route from monoclinic → tetragonal → cubic cannot occur (see Fig. 5). We recorded the Raman spectra of the high-pressure sample irradiated with 1.5×10^{12} ions/cm^2 outside the DAC (Fig. 9). Most interestingly, the sample irradiated at 23 GPa consists after quenching predominantly of the orthorhombic-II phase (small monoclinic residues exist at 178 and 190 cm^{-1}, but the fraction is low). The bands of the orthorhombic-II phase are highlighted by dotted lines in Fig. 9 (b). The strongest peaks of this structure are located at 160 and 432 cm^{-1} in agreement with earlier observations when ZrO_2 was quenched from 40 and 60 GPa [19, 26]. The finding of the orthorhombic-II phase is surprising because, at 23 GPa, ZrO_2 exists in its first high-pressure polymorph orthorhombic-I and is still ∼ 7 GPa away from the transition boundary to the orthorhombic-II phase. Irradiation with swift heavy ions obviously triggers the creation of this phase at a significantly lower pressure. Once produced, the orthorhombic-II phase is quenchable to ambient pressure. Pressure alone as the origin of the transformation into the orthorhombic-II phase was excluded by quenching a reference sample from 24 GPa, which rested there for one week, and did not show any orthorhombic-II signal (see Fig. 9 (a)). For pressures larger than ∼ 20 GPa, orthorhombic-II is the only possible high-temperature structure (see Fig. 5). It cannot be distinguished if the ion-beam induced transition proceeds via the temperature or pressure route.

Samples pressurized to 38 or 70 GPa are in the orthorhombic-II phase. Having no neighboring phase boundary, it is not surprising that the initial orthorhombic-II structure is preserved after irradiation (see Fig. 9 (c and d)). Due to the high bulk modulus of the orthorhombic-II structure (≥ 300 GPa [62]) and the principle characteristic of ZrO_2, it is considered as a good candidate for a new superhard material [62]. Since a fluence of 1.5×10^{12} U-ions/cm^2 has no influence on the orthorhombic-II structure, this high-pressure polymorph might be better suited for applications instead of the ambient pressure polymorphs. To validate this, irradiations of the orthorhombic-II structure with high ion fluences are planned.

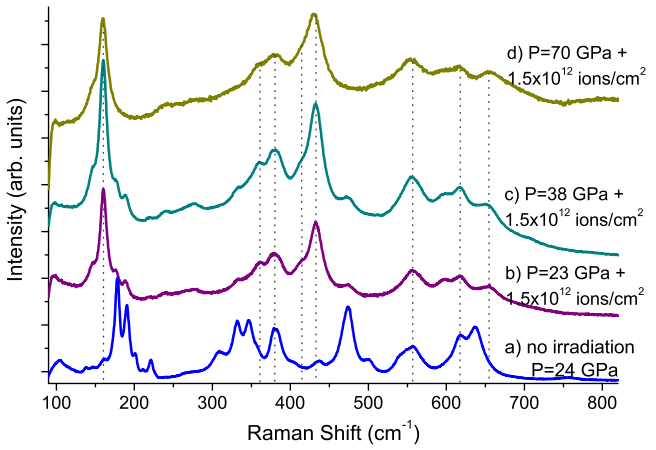

Figure 9: Raman analysis at ambient pressure of ZrO_2 irradiated with 1.5×10^{12} U-ions/cm^2 at 23 GPa (b), 38 GPa (c), and 70 GPa (d). Additionally a pressure reference (pristine ZrO_2 quenched from 24 GPa (a)).

4. Conclusions

In this study, the structural behavior of ZrO_2 has been investigated under ion irradiation at different pressures. We demonstrate that high-fluence irradiations at ambient pressure results in a transformation from the monoclinic to the high-temperature tetragonal phase. After quenching, the tetragonal phase can be stabilized. For heavy ions such as Au, Pb, and U, the monoclinic-to-tetragonal transformation requires a multiple-impact process, in agreement with earlier findings for medium mass ions [5, 63]. For irradiations at pressure around 10 GPa, the ion fluences needed for this transformation are more than one order of magnitude smaller than at ambient pressure. External pressure seems to induce sufficient strain to trigger the transformation process without track overlap. XRD spectroscopy of pressurized samples reveals that the transformation is not a direct monoclinic $\rightarrow$ tetragonal transition but takes a side route via the cubic phase. At pressures above > 20 GPa, the two high-temperature polymorphs are no longer accessible. The irradiation provokes a transition into the second high-pressure phase which can be quenched to ambient pressure. This orthorombic-II phase seems to be quite radiation resistant, making it interesting for further radiation hardness tests. Obviously, the combination of high pressure and heavy ions plays an important role in phase transformation processes including pressure-enhanced radiation effects as well as pressure effects enhanced by radiation.

5. Acknowledgements

The authors thank Dr. O. Seeck from the German Electron Synchrotron (DESY), Hamburg, Germany, for his great support during synchrotron beamtimes.
Financial support from the German Science Foundation DFG (Project No. FU 308/12) is gratefully acknowledged.

References

[1] R. Fleischer, P. Price, R. Walker, Nuclear Tracks in Solids, University of California Press, 1975.
[2] M. Toulemonde, C. Trautmann, E. Balanzat, K. Hjort, A. Weidinger, Track formation and fabrication of nanostructures with MeV-ion beams, Nucl. Instr. Meth. B 216 (2004) 1–8.
[3] C. Trautmann, M. Toulemonde, K. Schwartz, J. Costantini, A. Müller, Damage structure in the ionic crystal LiF irradiated with swift heavy ions, Nucl. Instr. Meth. B 164-165 (2000) 365–376.
[4] K. Schwartz, C. Trautmann, T. Steckenreiter, O. Geiß, M. Krämer, Damage and track morphology in lif crystals irradiated with gev ions, Phys. Rev. B 58 (1998) 17.
[5] A. Benyagoub, F. Levesque, F. Couvreur, C. Gibert-Mougel, C. Dufour, E. Paumier, Evidence of a phase transition induced in zirconia by high energy heavy ions, Appl. Phys. Lett. 77 (2000) 3197.
[6] U. Glasmacher, M. Lang, H. Keppler, F. Langenhorst, R. Neumann, D. Schardt, C. Trautmann, G. Wagner, Phase transitions in solids stimulated by simultaneous exposure to high pressure and relativistic heavy ions, Phys. Rev. Lett. 96 (2006) 195701.
[7] M. Lang, F. Zhang, J. Zhang, J. Wang, B. Schuster, C. Trautmann, R. Neumann, U. Becker, R. Ewing, Nanoscale manipulation of the propertries of solids at high pressure with relatistic ions, Nature Materials 8 (2009) 793.
[8] M. Lang, F. Zhang, J. Lian, C. Trautmann, R. Neumann, R. Ewing, Irradiation-induced stabilization of zircon ($ZrSiO_4$) at high pressure, Earth Planet. Sci. Lett. 269 291–295.
[9] B. Schuster, M. Lang, R. Klein, C. Trautmann, R. Neumann, A. Benyagoub, Structural phase transition in ZrO_2 induced by swift heavy ion irradiation at high pressure, Nucl. Instr. Meth. B 267 (2009) 964.
[10] J. Seydel, Nanokristallines Zirkoniumdioxid für Hochtemperatur-Brennstoffzellen, Ph.D. thesis, Technische Universität Darmstadt (2003).
[11] V. Oversby, C. McPheeters, C. Degueldre, J. Paratte, Control of civilian plutonium inventories using burning in a non-fertile fuel, J. Nucl. Mat. 245 (1997) 17–26.
[12] C. Degueldre, C. Hellwig, Study of a zirconia based inert matrix fuel under irradiation, J. Nucl. Mat. 320 (2003) 96–105.
[13] K. Sickafus, H. Matzke, K. Yasuda, J. Valdez, P. C. III, M. Nastasi, R. Verrall, Radiation damage effects in zirconia, J. Nucl. Mat. 274 (1999) 66–77.
[14] W. Gong, W. Lutze, R. Ewing, Zirconia ceramics for excess weapons plutoium waste, J. Nucl. Mat. 277 (2000) 239–249.
[15] W. Gong, W. Lutze, R. Ewing, Reaction sintered glass: a durable matrix for spinel-forming nuclear waste composition, J. Nucl. Mat. 278 (2000) 73–84.
[16] A. Benyagoub, Evidence of an ion-beam induced crystalline-to-crystalline phase transformation in hafnia, Euro. Phys. B 34 (2003) 395–398.
[17] J. Eichler, U. Eisele, J. Rödel, Mechanical propoerties of monoclinic zirconia, J. Am. Ceram. Soc. 87 (2004) 1401–1403.
[18] O. Ohtaka, E. Ito, S. Kume, Synthesis and phase stability of cotunnite-type zirconia, J. Am. Ceram. Soc. 71 (1988) 448–449.
[19] H. Arashi, T. Yagi, S. Akimoto, Y. Kuhdoh, New-high-pressure phase of ZrO_2 above 35 GPa, Phys. Rev. B 41 (1990) 7.
[20] J. Lowther, J. Dewhurst, Relative stability of ZrO_2 and HfO_2 structural phases, Phys. Rev. B 60 (1999) 21.
[21] J. Haines, J. Leger, A. Atouf, Crystal structure and equation of state of cotunnite type zirconia, J. Am. Ceram. Soc. 78 (1995) 445–448.
[22] P. Bouvier, G. Lucazeau, Raman spectra and vibrational analysis of nanometric tetragonal zirconia under high pressure, J. Phys. Chem. Solids 61 (2000) 569–578.
[23] C. Howard, R. Hill, B. Reichert, Structures of the ZrO_2 polymorphs at room temperature by high-resolution neutron powder diffraction, Acta Cryst. B 44 (1988) 116–120.
[24] O. Ohtaka, H. Fukui, T. Kunisada, T. Fujisawa, Phase relations and equations of state of ZrO_2 under high temperature and high pressure, Phys. Rev. B 63 (2001) 174108.
[25] O. Ohtaka, D. Andrault, Phase relations and equations of state of ZrO_2 to 100 GPa, J. Appl. Cryst. 38 (2005) 727–733.
[26] S. Desgreniers, K. Lagarec, High-density ZrO_2 and HfO_2 : Crystalline structures and equation of state, Phys. Rev. B 59 (1999) 13.
[27] J. Leger, P. Tomaszewski, A. Atouf, A. Pereira, Pressure-induced structural phase transition in zirconia under high pressure, Phys. Rev. B 47 (1993) 21.

[28] P. Bouvier, E. Djurado, G. Lucazeau, High-pressure structural evolution of undoped tetragonal nanocrystalline zirconia, Phys. Rev. B 62 (2000) 13.
[29] J. Haines, J. Leger, S. Hull, J. Petitet, A. Pereira, C. Perottoni, J. da Jornada, Characterization of the cotunnite-type phases of zirconia and hafnia by neutron diffraction and Raman spectroscopy, J. Am. Ceram. Soc. 80 (1997) 1910–1914.
[30] J. A. Valdez, M. Tang, Z. Chi, M. I. Peters, K. E. Sickafus, Characterization of an ion irradiation induced phase transformation in monoclinic zirconia, Nucl. Instr. and Meth. B 218 (2004) 103–110.
[31] J. Valdez, Z. Chi, K. Sickafus, Light ion irradiation-induced phase transformationin the monoclinic polymorph of zirconia, J. Nucl. Mater. 381 (2008) 259–266.
[32] D. Simeone, D. Gosset, J. Bechade, A. Chevarier, Analysis of the monoclinic-tetragonal phase transition of zirconia under irradiation, J. Nucl. Mat. 300 (2002) 27–38.
[33] D. Simeone, J. Bechade, D. Gosset, A. Chevarier, P. Daniel, H. Pilliaire, G. Baldinozzi, Investigation on the zirconia phase transition under irradiation, J. Nucl. Mat. 281 (2000) 171–181.
[34] A. Benyagoub, Mechanism of the monoclinic-to-tetragonal phase transition induced in zirconia and hafnia by swift heavy ions, Phys. Rev. B 72 (2005) 094114.
[35] A. Benyagoub, Kinetics of the crystalline to crystalline phase transformation induced in pure zirconia by swift heavy ion irradiation, Nucl. Instr. Meth. B 206 (2003) 132–138.
[36] G. Baldinozzi, D. Simeone, D. Gosset, I. Monnet, S. L. Caër, L. Mazerolles, Evidence of extended defects produced in pure zirconia irradiated by swift heavy ions, Phys. Rev. B 74 (2006) 132107.
[37] D. Simeone, G. Baldinozzi, D. Gosset, S. L. Caër, L. Mazerolles, I. Monnet, S. Bouffard, Effect of the energy deposition modes on the structural stability of pure zirconia, Nucl. Instr. Meth. B 266 (2008) 3023–3026.
[38] C. Gibert-Mougel, F. Couvreur, J. Costantini, S. Bouffard, et al., Phase transition of polycrysralline zirconia induced by swift heavy ion irradiation, J. Nucl. Mat. 295 (2001) 121–125.
[39] J.-M. Costantini, A. Kahn-Harari, F. Beuneu, F. Couvreur, Thermal annealing study of swift heavy-ion irradiated zirconia, J. Appl. Phys. 99 (2006) 123501.
[40] A. Benyagoub, Phase transformations in oxides induced by swift heavy ions, Nucl. Instr. Meth. B 245 (2006) 225–230.
[41] J. Ziegler, J. Biersack, The stopping and the Range of Ions in Matter SRIM-2008, http://www.srim.org, 2008.
[42] L. Merrill, W. A. Bassett, Miniature diamond anvil cell for single-crystal x-ray diffraction studies, Rev. Sci. Instr. 45 (1974) 290–294.
[43] R. Miletich, D. R. Allan, W. F. Kuhs, High-pressure single crystal techniques, in: High-temperature and high-pressure crystal chemistry, 2000, pp. 445–519.
[44] S. Klotz, J.-C. Chervin, P. Munsch, G. L. Marchand, Hydrostatic limits of 11 pressure transmitting media, J. Phys. D: Appl. Phys 42 (2009) 075413.
[45] H. Mao, J. Xu, P. Bell, Calibration of the ruby pressure gauge to 800 kbar under quasi-hydrostatic conditions, J. Geophys. Res. 91 (1968) 4673.
[46] H. Mao, P. Bell, J. Shaner, D. Steinberg, Specific volume measurements of Cu, Mo, Pd, and Ag and calibration of the ruby R1 fluorescence pressure gauge from 0.06 to 1 Mbar, J. Appl. Phys. 49 (1978) 3276.
[47] B. Schuster, C. Weikusat, R. Miletich, C. Trautmann, R. Neumann, F. Fujara, Influence of radiation damage on ruby as pressure gauge, Phys. Rev. B 82 (2010) 184110.
[48] M. Lang, U. Glasmacher, R. Neumann, D. Schardt, C. Trautmann, G. Wagner, Energy loss of 50-GeV uranium ions in natural diamond, Appl. Phys. A 80 (2005) 691.
[49] A. Hammersley, Fit2d: An introduction and overview, ESRF Internal Report (1997) ESRF97HA02T.
[50] L. Lutterotti, MAUD-Material Analysis Using Diffraction Programm, http://www.ing.unitn.it/ maud/, 2010.
[51] B. Toby, Expgui, a graphical user interface for GSAS, J. Appl. Cryst. 34 (2001) 210–213.
[52] M. Wojdyr, Fityk: a general-purpose peak fitting program, J. Appl. Cryst. 43 (2010) 1126–1128.
[53] B. Kim, J. Hahn, K. R. Han, Quantitative phase analysis in tetragonal-rich tetragonal/monoclinic two phase zirconia by Raman spectroscopy, J. Mat. Sci. Lett. 16 (1997) 669–671.
[54] W. Weber, Models and mechanisms of irradiation-induced amorphization in ceramics, Nucl. Instr. Meth. B 166-167 (2000) 98.
[55] J. Jagielski, L. Thomé, Damage accumulation in ion-irradiated cermics, Vacuum 81 (2007) 1352–1356.
[56] J. Gibbons, Ion implantation in semiconductors-part II: Damage production and annealing, Proc. IEEE 60 (1972) 1062.
[57] D. Smith, H. Newkirk, The crystal structure of baddeleyite (monoclinic ZrO_2) and its relation to the polymorphism of ZrO_2, Acta Cryst. 18 (1965) 983.
[58] M. Contreras, H. Orozco, A. Medina-Flores, Structural analysis of yttria partially stabilized zirconia, Rev. Mex. Fisica S 1 (2009) 127–129.
[59] D. Simeone, G. Baldinozzi, D. Gosset, S. L. Caër, L. Mazerolles, I. Monnet, S. Bouffard, Impact of radiation defects on the strcutural stability of pure zirconia, Phys. Rev. B 70 (2004) 134116.
[60] A. Foster, V. Sulimov, F. L. Gejo, A. Shluger, R. Nieminen, Structure and electrical levels of point defects in monoclinic zirconia, Phys. Rev. B 64 (2001) 224108.
[61] R. Cowley, Structural phase transitions I: Landau theory, Advances in Physics 28 (1980) 1–110.
[62] J. Lowther, Superhard materials, Phys. Stat. Sol. B 217 (2000) 533.
[63] D. Simeone, G. Baldinozzi, D. Gosset, S. L. Caër, Phase transformation of pure zirconia under irradiation: A textbook example, Nucl. Instr. Meth. B 250 (2006) 95–100.